(58) M. F. Hudson and K. M. Smith, *J. Chem. Soc., Chem. Commun.*, 515 (1973).
(59) M. F. Hudson and K. M. Smith, *Tetrahedron Lett.*, 2223 (1974).
(60) S. S. Eaton, G. R. Eaton, and R. H. Holm, *J. Organomet. Chem.*, **39**, 179 (1972).
(61) W. Bhatti, M. Bhatti, S. S. Eaton, and G. R. Eaton, *J. Pharm. Sci.*, **62**, 1574 (1973).
(62) S. S. Eaton and G. R. Eaton, *J. Chem. Soc., Chem. Commun.*, 576 (1974).
(63) F. A. Cotton, *Acc. Chem. Res.*, **2**, 240 (1969).
(64) N. I. G. Gapotchenko, N. V. Alekseev, N. E. Kolobova, K. N. Anisimov, I. A. Ronova, and A. A. Johansson, *J. Organomet. Chem.*, **35**, 319 (1972).
(65) A. H. Corwin and J. G. Erdman, *J. Am. Chem. Soc.*, **68**, 2473 (1946).
(66) A. D. Adler, F. R. Longo, J. D. Finarelli, J. Goldmacher, J. Assour, and L. Korsakoff, *J. Org. Chem.*, **32**, 476 (1967).
(67) G. H. Barnett, M. F. Hudson, and K. M. Smith, *Tetrahedron Lett.*, 2887 (1973).
(68) E. Sletten, J. Sletten, and L. H. Jensen, *Acta Crystallogr., Sect. B*, **25**, 1330 (1969).
(69) J. De Meulenaer and H. Tompa, *Acta Crystallogr.*, **19**, 1014 (1965).
(70) W. R. Busing, K. O. Martin, and H. Levy, ORFLS, A Fortran Crystallographic Least-Squares Program, Report ORNL-TM-305, Oak Ridge National Laboratory, Oak Ridge Tenn.
(71) D. T. Cromer and D. Liberman, *J. Chem. Phys.*, **53**, 1891 (1970).
(72) D. T. Cromer, "International Tables for X-Ray Crystallography", Vol. IV, in press.
(73) J. Housty and J. Clastre, *Acta Crystallogr.*, **10**, 695 (1957).
(74) D. L. Cullen and E. F. Meyer, Jr., *J. Am. Chem. Soc.*, **96**, 2095 (1974).
(75) D. L. Cullen and E. F. Meyer, Jr., *Acta Crystallogr., Sect. B*, **29**, 2507 (1973).

Binary Mixed Dioxygen Dinitrogen Complexes of Nickel, Palladium, and Platinum, $(O_2)M(N_2)_n$ (where M = Ni, Pd, or Pt; n = 1 or 2)

G. A. Ozin* and W. E. Klotzbücher

Contribution from the Lash Miller Chemistry Laboratories and Erindale College, University of Toronto, Toronto, Ontario, Canada. *Received November 25, 1974*

Abstract: The products of the cocondensation reactions of Ni, Pd, and Pt atoms with mixtures of O_2, N_2 and Ar at 6–10°K are investigated by matrix isolation infrared spectroscopy and are shown to be binary mixed dioxygen dinitrogen complexes of the form $(O_2)_xM(N_2)_y$. From the number and frequencies of the N–N and O–O stretching modes compared to the parent molecules $M(N_2)_n$ and $M(O_2)_m$ (where M = Ni, n = 1–4; M = Pd, Pt, n = 1–3; M = Ni, Pd, Pt, m = 1 or 2), their ligand concentration and warm-up behavior and $^{14}N_2$–$^{14}N^{15}N$–$^{15}N_2$–$^{16}O_2$–Ar and $^{16}O_2$–$^{16}O^{18}O$–$^{18}O_2$–$^{14}N_2$–Ar isotope multiplet patterns, the reaction products are established to be $(O_2)M(N_2)$ and $(O_2)M(N_2)_2$ containing "side-on" bonded dioxygen and "end-on" bonded dinitrogen in both complexes. Isotopic frequencies are computed for the ligand stretching and metal–ligand stretching modes of the individual complexes using a MVFF approximation and are found to be in close agreement with the observed values. The resulting bond stretching force constants enable one to gain a unique insight into the bonding of N_2 and O_2 to a transition metal in a situation where both ligands are competing for the same bonding electrons.

In a preliminary communication[1] we reported matrix infrared spectroscopic evidence for binary mixed dioxygen dinitrogen complexes of nickel formed in the cocondensation reactions of nickel atoms with $O_2/N_2/Ar$ mixtures. At that time, the mode of attachment of the O_2 and N_2 ligands to the metal had not been established. Moreover, the nature of the bonding of O_2 and N_2 simultaneously to a common metal atom remained an unanswered question. Since our original communication we have extended these experiments to include Pd and Pt and have been able to show that complexes of the form $(O_2)M(N_2)_n$ (where n = 1 or 2) exist for all members of the group. Without exception the complexes appear to contain dioxygen bonded in a side-on fashion and dinitrogen bonded in an end-on fashion to the central metal atom. Having obtained spectroscopic data for the complete group of complexes, we are now in a position to examine trends in their vibrational spectra, force constants, structures, stabilities, and bonding properties. In this paper we report such data.

Experimental Section

Monoatomic Ni and Pd vapors were generated by directly heating a 0.010-in. ribbon filament of the metal with ac in a furnace which has been described previously.[2] Platinum vapor was obtained by heating a 0.060-in. tungsten rod around the center of which were wound several turns of 0.010 in. Pt wire. The nickel, palladium, and platinum metal (99.99%) were supplied by McKay Inc., N.Y. Research grade $^{16}O_2$ (99.99%), $^{14}N_2$ (99.99%), and Ar (99.99%) were supplied by Matheson. Isotopically enriched $^{18}O_2$ (93%) was supplied by Miles Research Laboratories and $^{15}N_2$ (99.5%) by Prochem. Statistically scrambled mixtures of $^{16}O_2$–$^{16}O^{18}O$–$^{18}O_2$ and $^{14}N_2$–$^{14}N^{15}N$–$^{15}N_2$ were prepared by subjecting $^{16}O_2$–$^{18}O_2$ and $^{14}N_2$–$^{15}N_2$ mixtures of about 200 Torr to a continuous tesla discharge. The scrambling process and concentration ratios were monitored by gas phase Raman measurements.

The rate of metal atom deposition was continuously followed and controlled using a quartz crystal microbalance.[3a] The deposition rate was set such that the probability of a metal atom having another metal atom as nearest neighbor in the argon lattice was less than 10^{-3}. Matrix gas flows, controlled by a calibrated micrometer needle valve, were maintained in the range 2–8 mmol/hr. In the infrared experiments the matrices were deposited on a CsI window cooled to either 6°K by an Air Products liquid helium cryotip transfer system or to 12°K by means of an Air Products Displex closed cycle helium refrigerator. Ir spectra were recorded using Perkin-Elmer 621 and 180 spectrophotometers. Normal coordinate calculations were performed using a modified version of Schachtschneider's GMAT and EIGV programs for the MVFF analysis.[3b]

Results

The results for the $M(N_2)_n$ and $M(O_2)_m$ complexes have already been described in detail.[4–6] As some of the data are relevant to the present study, brief references to this earlier work will be necessary for a thorough appreciation of the $(O_2)M(N_2)_n$ problem. Each metal provides its own set of experimental difficulties and subtleties of spectral interpretation, so we will describe each in turn.

Nickel–Nitrogen Reactions. The spectrum obtained on depositing nickel atoms into a $^{14}N_2$:Ar = 1:100–1:200 matrix shows all the lines associated with the known com-

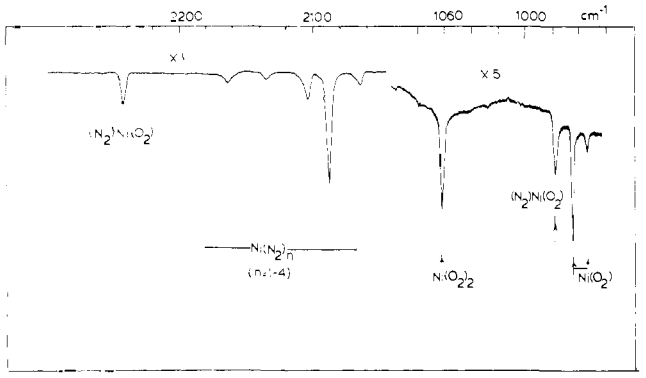

Figure 1. The matrix infrared spectrum of the products of the cocondensation reaction of nickel atoms with $^{16}O_2$:$^{14}N_2$:Ar ≃ 1:1:200 showing $Ni(N_2)_n$. $Ni(O_2)_m$ (where n = 1-4, m = 1-2), and $(O_2)Ni(N_2)$.

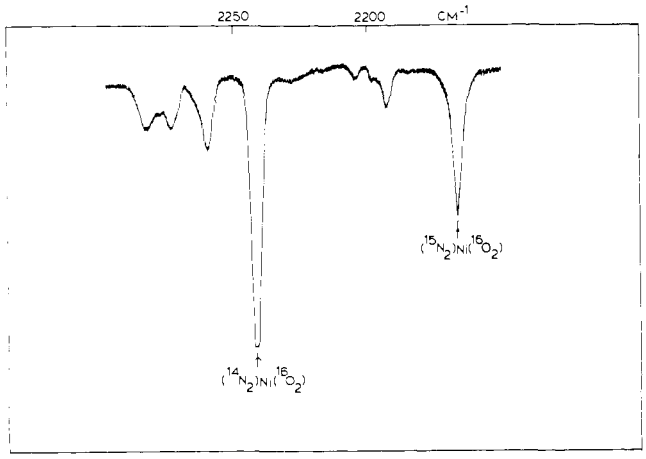

Figure 2. The matrix infrared spectrum of the products of the cocondensation reaction of nickel atoms with $^{16}O_2$:$^{14}N_2$:$^{15}N_2$:Ar ≃ 2:1:1:400 showing $(O_2)Ni(^{14}N_2)$ and $(O_2)Ni(^{15}N_2)$. The extra peaks belong to trace amounts of $(O_2)Ni(^{14}N_2)_2$, $(O_2)Ni(^{14}N_2)(^{15}N_2)$, and $(O_2)Ni(^{15}N_2)_2$ (see text).

pounds $Ni(N_2)$ (2088 cm^{-1}), $Ni(N_2)_2$ (2104 cm^{-1}), $Ni(N_2)_3$ (2134 cm^{-1}), and $Ni(N_2)_4$ (2174 cm^{-1}).[4] By carefully examining the Ni-N stretching region after matrix deposition and after matrix warm-up, it is possible to associate absorptions at 466, 406, 343, and 282 cm^{-1} with $Ni(N_2)$, $Ni(N_2)_2$, $Ni(N_2)_3$, and $Ni(N_2)_4$, respectively.[7]

Nickel-Oxygen Reactions. When nickel atoms are cocondensed with pure $^{16}O_2$, in addition to the 1062-cm^{-1} line previously assigned to the ν_{OO} stretching mode of $Ni(O_2)_2$, a weak feature is observed at 535 cm^{-1} which appeared to parallel the behavior of $Ni(O_2)_2$. In dilute $^{16}O_2$:Ar ≃ 1:10-1:100 mixtures the 965-cm^{-1} ν_{OO} stretching mode of $Ni(O_2)$ is observed together with a line at 507 cm^{-1}.[5] Warm-up experiments indicate that the 965 and 507 cm^{-1} absorptions are both associated with $Ni(O_2)$ and are assigned to ν_{OO} and ν_{NiO} stretching modes, respectively.[5]

Nickel-Oxygen-Nitrogen Reactions. When Ni atoms are cocondensed with $^{16}O_2$:$^{14}N_2$:Ar = 1:1:200 mixtures at 6-12°K, the infrared spectrum so obtained shows all of the lines associated with the known complexes $Ni(N_2)_n$ (n = 1-4), $Ni(O_2)_2$, and NiO_2 which are easily identified and will not be discussed further.

However, four new lines are observed, one in the NN stretching region at 2243 cm^{-1}, one in the ν_{OO} stretching region at 977 cm^{-1} (Figure 1), and two in the low frequency region at 478 cm^{-1} and 368 cm^{-1}.

Using $^{16}O_2$:$^{14}N_2$:$^{15}N_2$:Ar = 2:1:1:400 mixtures the single line originally at 2243 cm^{-1} becomes a doublet at 2243 and 2169 cm^{-1}, proving it to correspond to a species containing a single dinitrogen ligand (Figure 2). The line at 977 cm^{-1} remains unperturbed by the isotopic substitution. Similarly, the line originally at 977 cm^{-1} also becomes a doublet at 977 and 925 cm^{-1} when $^{16}O_2$:$^{18}O_2$:$^{14}N_2$:Ar = 1:1:2:400 mixtures are used, proving it to correspond to a species containing a single dioxygen molecule (Figure 3).

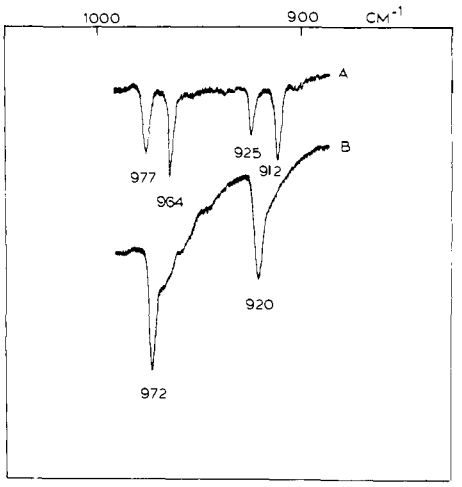

Figure 3. The matrix infrared spectrum, in the ν_{OO} stretching region, of the products of the cocondensation reaction of nickel atoms with $^{16}O_2$:$^{18}O_2$:$^{14}N_2$:Ar ≃ 1:1:2:400 (A) on deposition at 6-12°K showing $Ni(^{16}O_2)$, $Ni(^{18}O_2)$, $(^{16}O_2)Ni(^{14}N_2)$, and $(^{18}O_2)Ni(^{14}N_2)$ and (B) after warm-up to 30°K showing $(^{16}O_2)Ni(^{14}N_2)_2$ and $(^{18}O_2)Ni(^{14}N_2)_2$.

The weak low frequency mode at 368 cm^{-1} shows an isotopic counterpart at approximately 360 cm^{-1} whereas the line at 478 cm^{-1} appears unperturbed by $^{15}N_2$ isotopic substitution, implying that the absorption at about 368 cm^{-1} is probably best associated with a ν_{NiN} stretching mode. When $^{16}O_2$:$^{18}O_2$:$^{14}N_2$:Ar ≃ 1:1:2:400 mixtures are used, the weak line originally at 478 cm^{-1} appears to show a counterpart line at 468 cm^{-1} whereas the 368 cm^{-1} seems to be unperturbed by the $^{18}O_2$ isotopic substitution. These data support the above assignment for the ν_{NiN} stretching mode at 368 cm^{-1} and furthemore suggest that the 478-cm^{-1} line is probably associated with the stretching of a nickel-oxygen bond.

The mode of attachment of N_2 to a metal atom in MN_2 can be shown to be either end-on or side-on by using metal atom cocondensation reactions with statistical mixtures of nitrogen isotopes $^{14}N_2$:$^{14}N^{15}N$:$^{15}N_2$ = 1:2:1 diluted in Ar.[8] For *side-on* bonded N_2, three approximately equally spaced lines with absorption intensities in the ratio 1:2:1 are expected. For *end-on* bonded N_2, four lines with a closely spaced central doublet are expected with approximately equal absorption intensities. The central doublet in the latter is caused by the nonequivalence of the mixed isotopic $M^{14}N^{15}N$ and $M^{15}N^{14}N$.

Using a $^{16}O_2$:$^{14}N_2$:$^{14}N^{15}N$:$^{15}N_2$:Ar = 4:1:2:1:800 mixtures the line originally at 2243 cm^{-1} becomes a triplet at 2243, 2207, and 2169 cm^{-1}.

A high resolution scan of the line at 2207 cm^{-1} shows that it is in fact a doublet (Figure 4) with components at 2206.2/2207.0 cm^{-1}, establishing that the dinitrogen in the new complex is bonded in an end-on fashion to the nickel. Under the same conditions the $^{14}N^{15}N$ separation for NiN_2 was checked (Figure 4) and found to be in excellent agreement with the published value of 3.6 cm^{-1}.[9]

In $^{16}O_2$:$^{16}O^{18}O$:$^{18}O_2$:$^{14}N_2$:Ar = 1:2:1:4:300 experiments, the line originally at 977 cm^{-1} becomes a triplet at 977, 951, and 925 cm^{-1}. Under high resolution conditions the

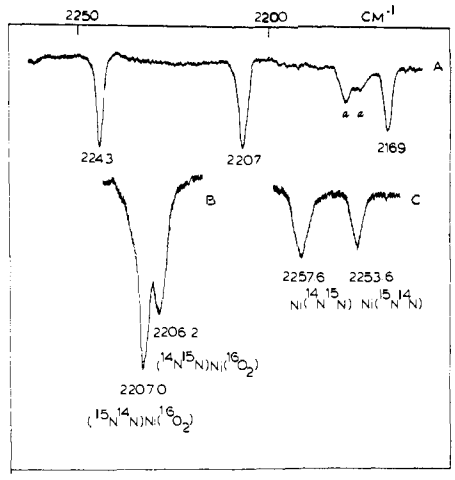

Figure 4. The matrix infrared spectrum (in the NN stretching region) of the products of the cocondensation reaction of nickel atoms with $^{16}O_2$:$^{14}N_2$:$^{14}N^{15}N$:$^{15}N_2$:Ar ≃ 4:1:2:1:800 showing (A) the isotopic lines of $(^{16}O_2)Ni(^nN^mN)$ (where n,m = 14 or 15) under low resolution conditions, (B) the $^{14}N^{15}N$ isotopic splitting of the central component (under high resolution) showing the inequivalence of the complexes $(^{16}O_2)Ni(^{14}N^{15}N)$–$(^{16}O_2)Ni(^{15}N^{14}N)$ depicting end-on bonded dinitrogen, and (C) and analogous isotopic splitting for $Ni(^{14}N^{15}N)$–$Ni(^{15}N^{14}N)$ (a = trace of $Ni(N_2)_4$).

line at 951 cm^{-1} remains a single line, consistent with the presence of "side-on" bonded dioxygen. A high resolution check on the 2243-cm^{-1} absorption in the scrambled oxygen isotope experiment shows that if there is an isotopic effect of the dioxygen ligand on the dinitrogen, the perturbation must be less than 0.8 cm^{-1}.

The data described above for *dilute* O_2–N_2–Ar matrices serve to characterize the new complex as one containing a single dinitrogen ligand bonded in an "end-on" fashion and a single dioxygen ligand bonded in a "side-on" fashion, to a single nickel atom, that is, mono(dioxygen)mono(dinitrogen)nickel $(O_2)Ni(N_2)$.

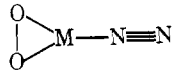

On allowing the original $^{16}O_2$:$^{14}N_2$:Ar = 1:1:200 matrix to warm up to 30–35°K, two new lines in the NN stretching region at 2282 and 2260 cm^{-1} grow in rapidly together with a single new line in the ν_{OO} stretching region at 972 cm^{-1} (Figures 5 and 6). The absorption at 959 cm^{-1} is a matrix split of NiO_2 in mixed matrices, its intensity depending on the matrix concentration and rate of deposition.[5]

The absorbances of the new lines continue to increase during warm-up experiments at the expense of the lines previously assigned to $(O_2)Ni(N_2)$ and strongly suggest that a second compound is being formed in a diffusion controlled reaction of the $(O_2)Ni(N_2)$ complex with N_2 in the matrix.

Using $^{16}O_2$–$^{14}N_2$–$^{15}N_2$–Ar mixtures, the modes originally at 2282 and 2260 cm^{-1} become a sextet pattern, showing three absorptions in the $^{14}N_2$ region at 2282, 2273, and 2260 cm^{-1} and three absorptions in the $^{15}N_2$ region at 2207, 2195, and 2183 cm^{-1}. These data prove that the species giving rise to the stretching modes at 2282 and 2260 cm^{-1} contains *two* dinitrogen ligands.

The ν_{OO} stretching mode originally at 972 cm^{-1} produces a doublet pattern at 972 and 920 cm^{-1} in $^{16}O_2$–$^{18}O_2$–$^{14}N_2$–Ar matrices (Figure 3B). On warming a $^{16}O_2$:$^{16}O^{18}O$:$^{18}O_2$:$^{14}N_2$:Ar = 1:2:1:4:300 matrix, besides the NN stretching modes at 2282 and 2260 cm^{-1}, a triplet of lines in the ν_{OO} stretching region at 972, 945, and 920 cm^{-1} is observed to grow in, establishing that the new species con-

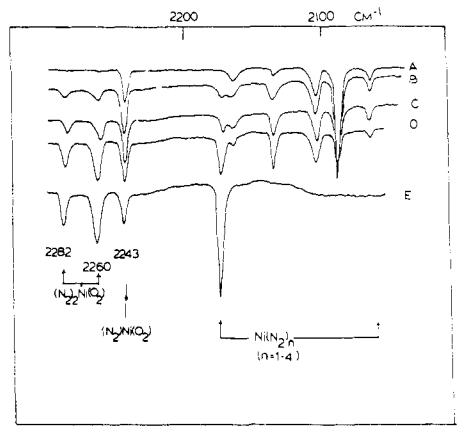

Figure 5. The matrix infrared spectrum in the NN stretching region of the products of the cocondensation reaction of nickel atoms with $^{16}O_2$:$^{14}N_2$:Ar ≃ 1:1:200: (A) on deposition at 6–12°K, (B) after warm-up to 15°K, (C) to 20°K, (D) to 25°K, and (E) to 30°K showing the matrix reaction of $(^{16}O_2)Ni(^{14}N_2)$ with $^{14}N_2$ to yield $(^{16}O_2)Ni(^{14}N_2)_2$.

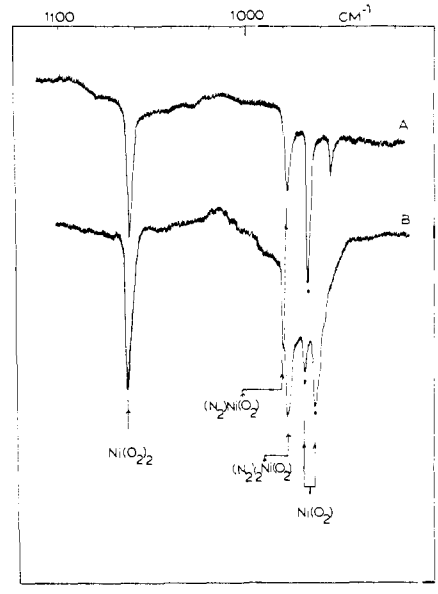

Figure 6. The same as Figure 5 but in the ν_{OO} stretching region (A) on deposition at 6–12°K and (B) after warm-up to 30°K. The asterisks indicate a known matrix splitting of $Ni(^{16}O_2)$.[5]

tains a single dioxygen ligand, most probably bonded in a side-on fashion to the nickel atom.

The intensity changes of the absorptions at 2282, 2260, and 972 cm^{-1} parallel each other during warm-up experiments and can be assigned to a single chemical species containing two dinitrogen and one dioxygen ligand coordinated to a single nickel atom, that is, bis(dinitrogen)mono(dioxygen)nickel, $(O_2)Ni(N_2)_2$. By comparison with $(O_2)Ni(N_2)$, the dioxygen is probably bonded in a side-on fashion, and the dinitrogens are most probably in an end-on fashion to the nickel atom:

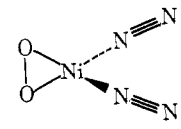

Using more concentrated mixtures containing scrambled dinitrogen $^{14}N_2$:$^{14}N^{15}N$:$^{15}N_2$:$^{16}O_2$:Ar = 1:2:1:4:80, one obtains on deposition a complicated spectrum containing information on all possible dinitrogen isotope combinations of $(^{16}O_2)Ni(^nN^mN)$ and $(^{16}O_2)Ni(^nN^mN)_2$, where n,m = 14

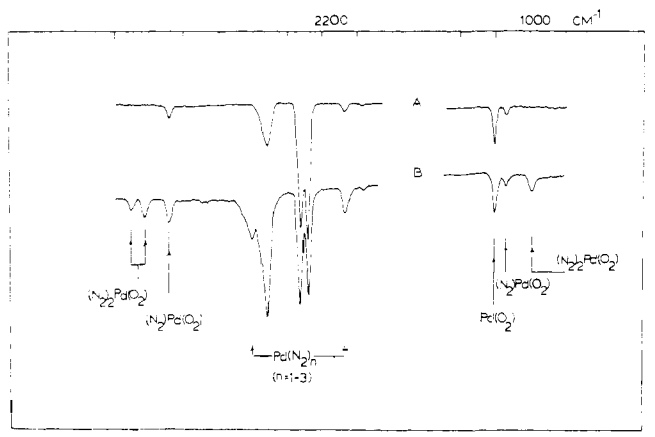

Figure 7. The matrix infrared spectrum of the products of the cocondensation reaction of palladium atoms with $^{16}O_2$:$^{14}N_2$:Ar ≃ 1:1:200 at 6–12°K (A) on deposition showing ($^{16}O_2$)Pd($^{14}N_2$) and (B) after warm-up to 20°K showing ($^{16}O_2$)Pd($^{14}N_2$)$_2$.

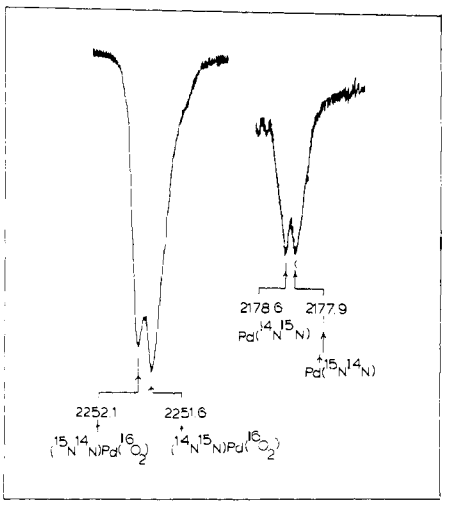

Figure 8. Matrix infrared spectrum in the NN stretching region, showing the $^{14}N^{15}N$ isotopic splitting and inequivalence of the molecules (A) ($^{16}O_2$)Pd($^{14}N^{15}N$)–($^{16}O_2$)Pd($^{15}N^{14}N$) and (B) Pd($^{14}N^{15}N$)–Pd($^{15}N^{14}N$), depicting in both cases "end-on" bonded dinitrogen.

or 15. Most of these lines are identified in Table V and provide useful additional data to help with the determination of the molecular force fields.

It is worth noting that when experiments were conducted using higher concentration ratios of O_2:N_2:Ar up to 1:2:30, absorption lines which could be attributed to a higher species than $(O_2)Ni(N_2)_2$ were *not* observed.

Palladium–Nitrogen Reactions. The spectrum obtained on depositing palladium atoms into a pure dinitrogen matrix at 6–12°K shows the two lines previously assigned to $Pd(N_2)_3$ at 2246/2238 cm^{-1} together with a single line in the PdN stretching region at 346 cm^{-1}.[7]

In a $^{14}N_2$/Ar = 1/15 matrix, all of the lines assigned to the known species $Pd(N_2)$ (2212/2208, 378/363 cm^{-1}) and $Pd(N_2)_2$ (2232; 339 cm^{-1}) can be observed in the initial deposition.[4,7] No evidence for species higher than $Pd(N_2)_3$ can be found.

Palladium–Oxygen Reactions. The spectrum obtained on depositing Pd atoms into pure $^{16}O_2$ matrices at 6°K shows the ν_{OO} stretching mode associated with $Pd(O_2)_2$ at 1108 cm^{-1} and a PdO stretching mode at 503 cm^{-1}.[5]

In $^{16}O_2$/Ar = 1/50 matrices, the infrared spectrum shows absorptions at 1024/422 cm^{-1} for $Pd(O_2)$ and 1108/504 cm^{-1} for $Pd(O_2)_2$. The line at 422 cm^{-1} can be associated with a PdO stretching mode of $Pd(O_2)$.[5]

Palladium–Oxygen–Nitrogen Reactions. The spectrum obtained on depositing palladium atoms into dilute $^{16}O_2$:$^{14}N_2$:Ar = 1:1:20–1:1:200 matrices at 6–12°K shows all of the lines associated with the known species PdN_2, $Pd(N_2)_2$ and PdO_2, $Pd(O_2)_2$.[5] Particularly noteworthy is the observation of a new line in the NN stretching region at 2288 cm^{-1} together with a new line in the ν_{OO} stretching region at 1014 cm^{-1} (Figure 7).

If these absorptions are associated with a complex containing a single dinitrogen ligand, $^{15}N_2$ isotopic substitution would shift the NN stretching mode at 2288 cm^{-1} very near to the mono(dinitrogen)palladium absorption at 2212/2208 cm^{-1}. Therefore a mixture of $^{16}O_2$:$^{15}N_2$:Ar = 2:1:100 was used. Besides the absorptions of the known complexes $Pd^{15}N_2$, $Pd(^{15}N_2)_2$, PdO_2, and $Pd(O_2)_2$, a single new line was observed at 2214 cm^{-1} as well as the previously mentioned line at 1014 cm^{-1}.

Using a $^{16}O_2$:$^{14}N_2$:$^{15}N_2$:Ar = 2:1:1:100 mixture in careful warm-up experiments, one can induce most of the $Pd^{14}N_2$ and $Pd^{15}N_2$ to react with free dinitrogen in the matrix. The 2288 and 2214-cm^{-1} lines *remain*, proving that the line at 2288 cm^{-1} belongs to a species containing a single dinitrogen ligand. Using a $^{16}O_2$:$^{14}N_2$:$^{14}N^{15}N$:$^{15}N_2$:Ar = 8:1:14:3:120 mixture, the line originally at 2288 cm^{-1} becomes a triplet at 2288, 2251, and 2214 cm^{-1}.

Examination of the 2251-cm^{-1} central isotope component under high resolution conditions shows it to be a doublet at 2251.6 and 2252.1 cm^{-1} (Figure 8), proving the dinitrogen in the mono(dinitrogen) palladium complex to be "end-on" bonded with a $^{14}N^{15}N$ isotopic split of approximately 0.5 cm^{-1}. Under the same conditions the $^{14}N^{15}N$ isotopic split for PdN_2 was found to be approximately 0.7 cm^{-1} (Figure 8). In none of the experiments described above was an isotopic effect observed on the ν_{OO} stretching mode at 1014 cm^{-1}.

On cocondensing Pd atoms with $^{14}N_2$:$^{16}O_2$:$^{16}O^{18}O$:$^{18}O_2$:Ar matrices, the absorption originally at 1014 cm^{-1} becomes a triplet at 1014, 986 and 960 cm^{-1}, proving that the line at 1014 cm^{-1} corresponds to a species containing a single dioxygen ligand. Although the signal-to-noise conditions were not ideal for high resolution scans of these weak oxygen isotope lines, the central component of the triplet remained unresolved and by analogy with $(O_2)Ni(N_2)$ can be taken to indicate the presence of side-on bonded dioxygen.

The data described above, as well as those from warm-up experiments, serve to characterize the new complex as containing a single dinitrogen bonded in an "end-on" fashion and a single dioxygen bonded in a "side-on" fashion to a single palladium atom, that is, mono(dinitrogen)mono(dioxygen)palladium, $(O_2)Pd(N_2)$.

On allowing the original $^{16}O_2$:$^{14}N_2$:Ar = 1:1:200 matrix to warm up slowly to 30°K, *two* new lines grow in the NN stretching region at 2310 and 2304 cm^{-1} together with a single new line in the ν_{OO} stretching region at 998 cm^{-1} (Figure 7).

In a pure $^{16}O_2$:$^{14}N_2$ = 1:1 matrix the two new lines occur on deposition at 2308 and 2300 cm^{-1}. They are fairly strong, as in the line at 998 cm^{-1}. Under these conditions the absorptions at 2288 and 1014 cm^{-1}, assigned to $(O_2)Pd(N_2)$, are absent. The data are therefore consistent with the formation of a second compound which is clearly very unstable, as warming the matrix to 20°K results in a decrease in intensity of the three lines at 2308, 2300, and 998 cm^{-1}. At 25°K all lines belonging to mixed dioxygen dinitrogen complexes have essentially disappeared.

When $^{16}O_2$–$^{14}N_2$–$^{15}N_2$–Ar mixtures are used, a complex spectrum is obtained. Band overlap of the new complexes with those of the mixed isotopic complexes of $Pd(N_2)_2$ and

$Pd(N_2)_3$ is unavoidable. The best results are found on depositing Pd atoms into a 1:1:1:10 mixture followed by careful warm-up experiments. Under these conditions, most of the $Pd(^{14}N_2)_n(^{15}N_2)_{2-n}$ complexes disappear and only the absorptions of the $Pd(^{14}N_2)_n(^{15}N_2)_{3-n}$ complexes can be observed. The remaining spectrum shows lines in the $^{14}N_2$ region at 2310 and 2308 cm^{-1} and lines in the $^{15}N_2$ region at 2233 and 2229 cm^{-1}.

These data prove that the species giving rise to the stretching modes at 2310/2304 cm^{-1} in mixed dioxygen-dinitrogen matrices contain *two* dinitrogen ligands. In all the experiments with dinitrogen substitution, perturbation of the absorption in the ν_{OO} stretching region was not observed.

Let us consider the overlap complications which can arise in $^{16}O_2$–$^{16}O^{18}O$–$^{18}O_2$ isotopic substitution experiments. With an isotopic shift of ca. 54 cm^{-1} for $^{18}O_2$ substitution and approximately half this value for $^{16}O^{18}O$, the predicted spectrum will be something like the following.

	PdO_2	$(O_2)Pd(N_2)$	$(O_2)Pd(N_2)_2$
$\nu^{16}O^{16}O$	1022	1014	998
$\nu^{16}O^{18}O$	993	988	970
$\nu^{18}O^{18}O$	963	960	942

With these figures in mind, palladium atoms were cocondensed with a concentrated $^{16}O_2$:$^{18}O_2$:$^{14}N_2$ = 1:1:8 mixture and warmed to 20°K. The spectrum shows that $Pd(O_2)$ and $(O_2)Pd(N_2)$ are absent. The line originally at 998 cm^{-1} becomes a doublet at 998 and 942 cm^{-1}, indicating that the species giving rise to these absorptions contains only a single dioxygen ligand. Using a mixture of $^{16}O_2$:$^{16}O^{18}O$:$^{18}O_2$:$^{14}N_2 \simeq$ 1:2:1:4, three weak lines are observed at 998, 970, and 942 cm^{-1} after warm-up to 20°K. No significant effects can be observed on the absorptions in the NN stretching region by isotopic dioxygen substitution. By comparison with $(O_2)Ni(N_2)_2$, the data described above serve to characterize the new complex as containing two dinitrogen ligands, probably coordinated in an "end-on" bonded fashion, and a single dioxygen ligand, probably coordinated in "side-on" bonded fashion, to a single palladium atom, that is, mono(dioxygen)bis(dinitrogen)palladium, $O_2Pd(N_2)_2$.

Platinum–Nitrogen Reactions. When platinum atoms are cocondensed with a pure nitrogen matrix at 6–12°K the infrared spectrum on deposition consists of two lines in the NN stretching region at 2217 and 2206 cm^{-1}, the latter being more intense. A line is observed in the Pt–N stretching region at 399 cm^{-1}. When this matrix is warmed to 30°K the line at 2217 cm^{-1} grows at the expense of the absorption at 2206 cm^{-1}, the low mode remaining essentially unchanged. These results are essentially identical with those obtained previously for $Pt(N_2)_3$.[6] When a $^{14}N_2$:Ar $\simeq$ 1:10 mixture is used, the spectrum shows three lines, a closely spaced doublet at 2172/2168 cm^{-1} and a single line at 2197.5 cm^{-1}. In the Pt–N stretching region two lines are observed at 394 and 360 cm^{-1}. The intensities of the absorptions at 2172/2168, 394 cm^{-1} and 2197.5, 360 cm^{-1} parallel each other during warm-up experiments and have been assigned to the complexes $Pt(^{14}N_2)$ and $Pt(^{14}N_2)_2$, respectively.[6,7]

Platinum–Oxygen Reactions. The spectrum obtained on depositing Pt atoms into a pure $^{16}O_2$ matrix at 6–12°K shows a closely spaced doublet at 1052.6/1049.2 cm^{-1}.[5] On warming the matrix to 30°K, the relative intensities of the components of this doublet change and shift to 1049.8/1048.8 cm^{-1}. This effect has been observed previously and rationalized in terms of different matrix sites in the crystalline portions of the α and β phases of solid oxygen.[5] In dilute $^{16}O_2$–Ar mixtures, this absorption appears at 1050.0/1047.2 cm^{-1} together with a new doublet feature at 925.8/920.8 cm^{-1}. In none of these experiments is it possible to observe metal-ligand stretching modes even under conditions of high expansion. Oxygen isotopic substitution characterizes these dioxygen complexes as $Pt(O_2)_2$ and $Pt(O_2)$, respectively.[5]

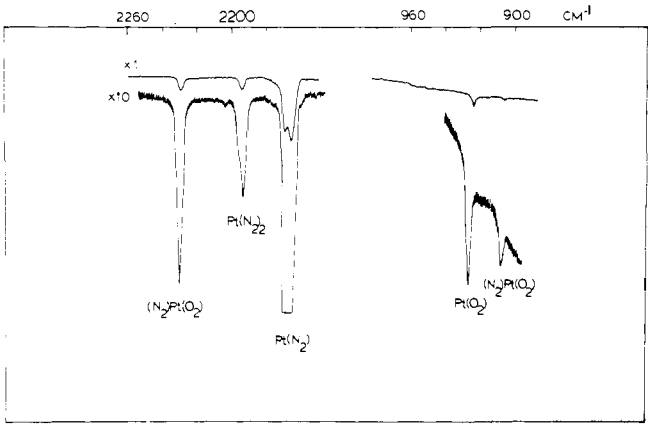

Figure 9. The matrix infrared spectrum of the products of the cocondensation reaction of platinum atoms with $^{16}O_2$:$^{14}N_2$:Ar $\simeq$ 1:1:50 showing, besides $Pt(^{14}N_2)$, $Pt(^{14}N_2)_2$, and $Pt(^{16}O_2)$, absorptions belonging to the new complex $(^{16}O_2)Pt(^{14}N_2)$.

Platinum–Oxygen–Nitrogen Reactions. When platinum atoms are cocondensed with a mixture of $^{16}O_2$:$^{14}N_2$:Ar = 1:1:50 at 6–12°K, the infrared spectrum obtained after several hours deposition shows, besides the known absorptions for PtN_2, $Pt(N_2)_2$, $Pt(O_2)$, and $Pt(O_2)_2$, *four* new lines, one in the NN stretching region at 2229 cm^{-1}, one in the ν_{OO} stretching region at 909 cm^{-1}, and two in the PtN/PtO stretching region at 502 and 497 cm^{-1} (Figure 9). Because of overlap problems of the pure dinitrogen species in a $^{16}O_2$–$^{14}N_2$–$^{15}N_2$ experiment, a run was performed with a $^{16}O_2$:$^{15}N_2$:Ar = 1:1:25 mixture. The resulting spectrum showed lines at 2157 and 909 cm^{-1}.

A problem also arises with scrambled $^{16}O_2$–$^{14}N_2$–$^{14}N^{15}N$–$^{15}N_2$ isotope experiments. If the new species contains a single dinitrogen ligand, the $^{14}N^{15}N$ absorptions of the complex could shift under the 2197 cm^{-1} line of $Pt(^{14}N_2)_2$. With this complication in mind, the high resolution spectrum of Pt atoms cocondensed with a $^{14}N_2$:$^{14}N^{15}N$:$^{15}N_2$:$^{16}O_2$:Ar = 1:2:1:8:120 mixture shows, besides the known lines of the pure species, a three-line spectrum at 2231, 2195.5, and 2160 cm^{-1}. The 2195.5-cm^{-1} absorption can only be distinguished from the $Pt(^{14}N_2)_2$ line using a spectral resolution of 0.6 cm^{-1}. No significant perturbation is observed for the ν_{OO} stretching mode at 909 cm^{-1}.

Using a dilute $^{14}N_2$–$^{16}O_2$–$^{18}O_2$–Ar mixture, the spectra show, besides the known pure platinum oxygen features, a doublet at 909 and 860 cm^{-1}. With a $^{16}O_2$–$^{16}O^{18}O$–$^{18}O_2$–Ar mixture, a three-line spectrum is observed at 909, 883, and 860 cm^{-1}.

These data together with warm-up experiments prove that the absorptions at 2229 and 909 cm^{-1} are associated with a single complex containing one dioxygen and one dinitrogen ligand, that is, mono(dioxygen)mono(dinitrogen)-platinum, $(O_2(Pt(N_2)$. By analogy with Ni and Pd, the oxygen is probably bonded "side-on", the nitrogen "end-on", to the platinum.

Cocondensation of Pt atoms with a $^{16}O_2$:$^{14}N_2$ = 1:2 mixture results in small shifts of the absorptions of $Pt(O_2)_2$ and $Pt(N_2)_3$ from 1052/1049 to 1047/1035 cm^{-1} and 2217/2206 to 2219/2209 cm^{-1}, respectively. Particularly noteworthy are the *two* new lines which appear in the NN

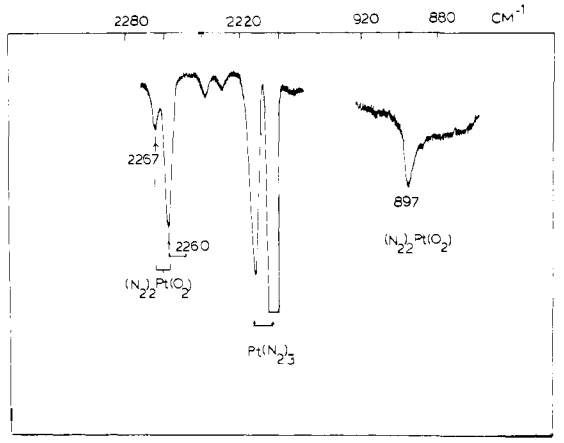

Figure 10. The matrix infrared spectrum of the products of the cocondensation reaction of platinum atoms with $^{16}O_2$:$^{14}N_2 \simeq 1{:}2$ showing, besides $Pt(N_2)_3$, absorptions belonging to the new complex $(^{16}O_2)Pt(^{14}N_2)_2$.

stretching region at 2267 and 2260 cm^{-1} (the latter being the more intense) together with a new line in the ν_{OO} stretching region at 897 cm^{-1} (Figure 10). In similar experiments using $^{15}N_2$ substitution, weak absorptions at 2188, 2181 cm^{-1} can be observed, as well as the line at 897 cm^{-1}.

When a $^{16}O_2$:$^{18}O_2$:$^{14}N_2$:Ar = 1:1:4:20 mixture is used, a *two*-line spectrum is observed in the OO stretching region at 897 and 848 cm^{-1}.

Due to the very low absorption coefficients for the ν_{OO} stretching modes, the spectrum obtained after depositing Pt atoms into a $^{16}O_2$:$^{16}O^{18}O$:$^{18}O_2$:$^{14}N_2$:Ar = 1:2:1:8:40 mixture is rather weak. Nevertheless it is possible to observe absorptions at 2267/2260 cm^{-1} in the NN stretching region and at 897, 872, and 848 cm^{-1} in the ν_{OO} stretching region. The scrambled $^{14}N_2$-$^{14}N^{15}N$-$^{15}N_2$-$^{16}O_2$-Ar mixture produces a complex spectrum in the NN stretching region, containing information on all possible dinitrogen isotopic combinations of $(^{16}O_2)Pt(^nN^mN)_2$, where n,m = 14 or 15 (Table VII).

The data described above serve to identify the lines at 2267/2260 and 897 cm^{-1} as belonging to a species containing a single dioxygen and two dinitrogen ligands, that is, mono(dioxygen)bis(dinitrogen)platinum, $(O_2)Pt(N_2)_2$. By analogy with the results for nickel and palladium, the oxygen is probably bonded in a "side-on" fashion and the dinitrogens in an "end-on" fashion to the platinum atom.

Normal Coordinate Calculations. The intermolecular forces in complexes, even those containing only a few atoms, are invariably complicated and can often only be calculated using approximate force fields. The method that has been successfully applied to carbonyl and dinitrogen complexes is the Cotton-Kraihanzel force field approximation[10] and is based on the ability to decouple the ligand stretching from the metal-ligand modes.

Preliminary calculations using the diatomic oscillator model showed that, for dioxygen compounds of the transition metals,[5] vibrational coupling between the metal-oxygen and the oxygen-oxygen stretching modes was appreciable and indicated that a more complete force field should be used. To allow direct comparison of force constants in the present study, all molecules were calculated using a MVFF approach and a modified version of Schachtschneider's GMAT and EIGV programs.[3b]

Mono(dioxygen) Mono(dinitrogen) Complexes of Ni, Pd, and Pt. Due to the lack of exact bond length data, calculations were performed on a model complex containing a side-on bonded dioxygen ligand and an end-on bonded dinitrogen ligand where the M—N≡N bond was assumed to be linear. The ligand and metal-ligand bond lengths were taken by comparison with literature data for stable dinitrogen and dioxygen complexes. In the calculations, all force

Table I. Observed and Calculated Frequencies of Isotopically Substituted $(^pO^qO)Ni(^nN^mN)$ (where n,m = 14 or 15 and p,q = 16 or 18)

Molecule	Obsd (cm^{-1})	Calcd (cm^{-1})	Mode	Molecule	Obsd (cm^{-1})	Calcd (cm^{-1})	Mode
$^{16}O_2Ni^{14}N_2$	977	978.1	ν_{O-O}	$^{16}O_2Ni^{15}N^{14}N$	977	978.0	ν_{O-O}
	478	478.4	ν_{M-O} (sym)		—	478.1	ν_{M-O} (sym)
	2243	2244.2	ν_{N-N}		2206.2	2206.0	ν_{N-N}
	368	367.4	ν_{M-N}		—	362.9	ν_{M-N}
$^{16}O_2Ni^{15}N_2$	977	978.1	ν_{O-O}	$^{18}O_2Ni^{14}N_2$	925	923.6	ν_{O-O}
	478	477.7	ν_{M-O} (sym)		468	464.7	ν_{M-O} (sym)
	2169	2168.1	ν_{N-N}		2243	2244.2	ν_{N-N}
	360	358.5	ν_{M-N}		—	362.0	ν_{M-N}
$^{16}O_2Ni^{14}N^{15}N$	977	978.1	ν_{O-O}	$^{16}O^{18}ONi^{14}N_2$	951	951.3	ν_{O-O}
	—	478.1	ν_{M-O} (sym)		—	471.7	ν_{M-O}
	2207	2207.0	ν_{N-N}		2244	2244.2	ν_{N-N}
	—	362.7	ν_{M-N}		—	366.5	ν_{M-N}

Table II. Observed and Calculated Frequencies of Isotopically Substituted $(^pO^qO)Pd(^nN^mN)$ (where n,m = 14 or 15 and p,q = 16 or 18)

Molecule	Obsd (cm^{-1})	Calcd (cm^{-1})	Mode	Molecule	Obsd (cm^{-1})	Calcd (cm^{-1})	Mode
$^{16}O_2Pd^{14}N_2$	1014	1014.8	ν_{O-O}	$^{16}O_2Pd^{15}N^{14}N$	1014	1014.8	ν_{O-O}
	418	416.0	ν_{M-O} (sym)		—	415.9	ν_{M-O} (sym)
	2288	2289.8	ν_{N-N}		2251.6	2251.1	ν_{N-N}
	366	365.1	ν_{M-N}		—	359.9	ν_{M-N}
$^{16}O_2Pd^{15}N_2$	1014	1014.8	ν_{O-O}	$^{18}O_2Pd^{14}N_2$	960	957.2	ν_{O-O}
	—	415.9	ν_{M-O} (sym)		398	399.9	ν_{M-O} (sym)
	2214	2212.2	ν_{N-N}		2289	2289.8	ν_{N-N}
	354	355.0	ν_{M-N}		—	362.1	ν_{M-N}
$^{16}O_2Pd^{14}N^{15}N$	1014	1014.8	ν_{O-O}	$^{16}O^{18}OPd^{14}N_2$	986	986.5	ν_{O-O}
	—	415.9	ν_{M-O} (sym)		—	408.9	ν_{M-O}
	2252.1	2251.6	ν_{N-N}		2289	2289.8	ν_{N-N}
	—	359.8	ν_{M-N}		—	365.3	ν_{M-N}

Table III. Observed and Calculated Frequencies of Isotopically Substituted ($^{p}O^{q}O$)Pt($^{n}N^{m}N$) (where n,m = 14 or 15 and p,q = 16 or 18)

Molecule	Obsd (cm^{-1})	Calcd (cm^{-1})	Mode	Molecule	Obsd (cm^{-1})	Calcd (cm^{-1})	Mode
$^{16}O_2Pt^{14}N_2$	909	910.2	ν_{O-O}	$^{16}O_2Pt^{15}N^{14}N$	909	910.2	ν_{O-O}
	—	392.2	ν_{M-O} (sym)		—	386.2	ν_{M-O} (sym)
	2229	2231.6	ν_{N-N}		2195.5	2193.9	ν_{N-N}
	—	346.5	ν_{M-N}		—	346.4	ν_{M-N}
$^{16}O_2Pt^{15}N_2$	909	910.2	ν_{O-O}	$^{18}O_2Pt^{14}N_2$	860	858.4	ν_{O-O}
	—	380.4	ν_{M-O} (sym)		—	391.7	ν_{M-O} (sym)
	2157	2156.0	ν_{N-N}		2229	2231.7	ν_{N-N}
	—	346.4	ν_{M-N}		—	329.4	ν_{M-N}
$^{16}O_2Pt^{14}N^{15}N$	909	910.2	ν_{O-O}	$^{16}O^{18}OPt^{14}N_2$	883	884.7	ν_{O-O}
	—	386.0	ν_{M-O} (sym)		—	391.9	ν_{M-O}
	2195.5	2194.5	ν_{N-N}		2229	2231.8	ν_{N-N}
	—	346.4	ν_{M-N}		—	340.3	ν_{M-N}

Table IV. Best Fit MVFF Force Constants[a] for $(O_2)M(N_2)$ (where M = Ni, Pd, or Pt)

	$(O_2)Ni(N_2)$	$(O_2)Pd(N_2)$	$(O_2)Pt(N_2)$
k_{NN}	20.90	21.92	20.91
k_{MN}	1.78	1.84	2.26
$k_{MN\cdot NN}$	0.59	0.77	0.95
$k_{NN\cdot OO}$	0.30	0.30	0.30
$k_{NN\cdot MO}$	0.01	0.01	0.01
$k_{MN\cdot MO}$	0.20	0.20	0.20
$k_{MN\cdot OO}$	0.01	0.01	0.01
k_{OO}	3.80	4.30	3.37
k_{MO}	1.57	1.48	1.20
$k_{OO\cdot MO}$	0.45	0.45	0.45
$k_{MO\cdot MO}$	0.40	0.24	0.22

[a] Units in mdyn/Å.

constants besides those associated with bond stretching and stretch-stretch interactions were assumed to be equal to zero. The results of these calculations are summarized in Tables I-IV.

Mono(dioxygen) Bis(dinitrogen) Complexes of Ni, Pd, and Pt. The experimental results described earlier indicate that in complexes containing one dioxygen and two dinitrogen ligands the dioxygen is bonded in a "side-on" fashion and the dinitrogens most probably in an "end-on" fashion to the metal atom. This is consistent with previous data which showed the dinitrogen ligands in $Ni(N_2)_n$ complexes to be end-on bonded while the dioxygen ligands in $Ni(O_2)_m$ complexes are side-on bonded. The data for the similar palladium and platinum complexes supported this view.

In our normal coordinate calculations for $(O_2)M(N_2)_2$, the bond length parameters were assumed to be the same as for the respective $(O_2)M(N_2)$ complexes. Our model assumes a pseudo-tetrahedral stereochemistry about the central metal atom with a bond angle of 110° between the dinitrogen ligands. The results of these calculations are summarized in Tables V-VIII.

Discussion

The following discussion of the bonding properties and stabilities of $(O_2)M(N_2)$ and $(O_2)M(N_2)_2$ rest heavily on our earlier considerations of the parent compounds $M(N_2)_n$ and $M(O_2)_m$.[4-6] Rather than reiterate the arguments presented previously, we have summarized the relevant frequency and force constant data for all complexes in Table IX.

In general, binary mixed dioxygen dinitrogen complexes tend to have higher NN stretching frequencies, yet essentially the same ν_{OO} stretching frequencies, as the parent

Table V. Observed and Calculated[a] Frequencies of Isotopically Substituted ($^{p}O^{q}O$)Ni($^{n}N^{m}N$)$_2$ (where n,m = 14 or 15 and p,q = 16 or 18)

Molecule	Obsd (cm^{-1})	Calcd (cm^{-1})	Mode	Molecule	Obsd (cm^{-1})	Calcd (cm^{-1})	Mode
$^{16}O_2Ni(^{14}N_2)_2$	972	972.7	ν_{O-O}	$^{16}O^{18}ONi(^{14}N_2)_2$	945	945.9	ν_{O-O}
	—	488.2	ν_{M-O} sym		2283	2283.3	ν_{N-N} sym
	2282	2283.3	ν_{N-N} sym		2260	2260.7	ν_{N-N} asym
	2260	2260.7	ν_{N-N} asym	$^{16}O_2Ni(^{14}N^{15}N)_2$	(2246)	2246.0	ν_{N-N} sym
	345	342.6	ν_{M-N} sym		(2226)	2223.4	ν_{N-N} asym
$^{16}O_2Ni(^{15}N_2)_2$	972	972.6	ν_{O-O}		—	338.1	ν_{M-N} sym
	—	486.9	ν_{M-O} sym	$^{16}O_2Ni(^{15}N^{14}N)_2$	(2246)	2243.9	ν_{N-N} sym
	2207	2205.9	ν_{N-N} sym		(2226)	2222.0	ν_{N-N} asym
	2183	2184.1	ν_{N-N} asym		—	338.4	ν_{M-N} sym
	—	334.0	ν_{M-N} sym	$^{16}O_2Ni(^{14}N_2)(^{14}N^{15}N)$	(2276)	2275.2	$\nu_{^{14}N-^{14}N}$
$^{18}O_2Ni(^{14}N_2)_2$	920	918.3	ν_{O-O}		(2234)	2231.6	$\nu_{^{14}N-^{15}N}$
	—	475.2	ν_{M-O} sym	$^{16}O_2Ni(^{14}N_2)(^{15}N^{14}N)$	(2276)	2274.9	$\nu_{^{14}N-^{14}N}$
	2283	2283.2	ν_{N-N} sym		(2234)	2230.0	$\nu_{^{15}N-^{14}N}$
	2260	2260.7	ν_{N-N} asym	$^{16}O_2Ni(^{14}N^{15}N)(^{15}N^{14}N)$	(2246)	2245.0	$\nu_{^{14}N-^{15}N}$
	—	337.5	ν_{M-N} sym		(2226)	2222.7	$\nu_{^{15}N-^{14}N}$
$^{16}O_2Ni^{14}N_2{}^{15}N_2$	972	972.6	ν_{O-O}	$^{16}O_2Ni(^{14}N^{15}N)(^{15}N_2)$	2236	2237.6	$\nu_{^{14}N-^{15}N}$
	—	487.5	ν_{M-O} sym		(2195)	2192.1	$\nu_{^{15}N-^{15}N}$
	2273	2273.6	$\nu_{^{14}N-^{14}N}$	$^{16}O_2Ni(^{15}N^{14}N)(^{15}N_2)$	(2236)	2235.9	$\nu_{^{15}N-^{14}N}$
	2195	2193.4	$\nu_{^{15}N-^{15}N}$		(2195)	2192.1	$\nu_{^{15}N-^{15}N}$
	—	348.9	$\nu_{M-^{14}N}$				
	—	337.8	$\nu_{M-^{15}N}$				

[a] Numbers in parentheses represent frequencies assigned after calculating their values. These frequencies were usually part of a complex overlapping band structure. This also applies to Tables VI and VII.

Table VI. Observed and Calculated Frequencies of Isotopically Substituted $(^{p}O^{q}O)Pd(^{n}N^{m}N)_2$ (where n,m = 14 or 15 and p,q = 16 or 18)

Molecule	Obsd (cm^{-1})	Calcd (cm^{-1})	Mode	Molecule	Obsd (cm^{-1})	Calcd (cm^{-1})	Mode
$^{16}O_2Pd(^{14}N_2)_2$	998	997.9	ν_{O-O}	$^{16}O^{18}OPd(^{14}N_2)_2$	970	970.0	ν_{O-O}
	—	439.8	ν_{M-O} sym		2311	2311.4	ν_{N-N} sym
	2310	2311.4	ν_{N-N} sym		2304	2304.5	ν_{N-N} asym
	2304	2304.5	ν_{N-N} asym	$^{16}O_2Pd(^{14}N^{15}N)_2$	—	997.8	ν_{O-O}
	—	355.6	ν_{M-N} sym		(2272)	2273.5	ν_{N-N} sym
$^{16}O_2Pd(^{15}N_2)_2$	998	997.8	ν_{O-O}		(2264)	2266.4	ν_{N-N} asym
	—	438.0	ν_{M-O} sym	$^{16}O_2Pd(^{15}N^{14}N)_2$	—	997.8	ν_{O-O}
	2233	2233.1	ν_{N-N} sym		(2272)	2271.7	ν_{N-N} sym
	—	2226.4	ν_{N-N} asym		(2264)	2265.3	ν_{N-N} asym
	—	346.4	ν_{M-N} sym	$^{16}O_2Pd(^{14}N_2)(^{14}N^{15}N)$	(2309)	2308.3	$\nu_{^{14}N-^{14}N}$
$^{18}O_2Pd(^{14}N_2)_2$	942	941.3	ν_{O-O}		(2270)	2269.6	$\nu_{^{14}N-^{15}N}$
	—	426.7	ν_{M-O} sym	$^{16}O_2Pd(^{14}N_2)(^{15}N^{14}N)$	(2309)	2308.2	$\nu_{^{14}N-^{14}N}$
	2310	2311.3	ν_{N-N} sym		(2270)	2268.2	$\nu_{^{15}N-^{14}N}$
	2304	2304.5	ν_{N-N} asym	$^{16}O_2Pd(^{14}N^{15}N)(^{15}N^{14}N)$	(2270)	2272.7	$\nu_{^{14}N-^{15}N}$
	—	349.8	ν_{M-N} sym		(2264)	2265.8	$\nu_{^{15}N-^{14}N}$
$^{16}O_2Pd(^{14}N_2)(^{15}N_2)$	998	997.9	ν_{O-O}	$^{16}O_2Pd(^{14}N^{15}N)(^{15}N_2)$	(2270)	2270.2	$\nu_{^{14}N-^{15}N}$
	—	439.1	ν_{M-O}		(2230)	2229.5	$\nu_{^{15}N-^{15}N}$
	2308	2308.1	$\nu_{^{14}N-^{14}N}$	$^{16}O_2Pd(^{15}N^{14}N)(^{15}N_2)$	(2270)	2268.8	$\nu_{^{15}N-^{14}N}$
	2229	2229.6	$\nu_{^{15}N-^{15}N}$		(2230)	2229.5	$\nu_{^{15}N-^{15}N}$
	—	359.8	$\nu_{M-^{14}N}$				
	—	348.7	$\nu_{M-^{15}N}$				

Table VII. Observed and Calculated Frequencies of Isotopically Substituted $(^{p}O^{q}O)Pt(^{n}N^{m}N)_2$ (where n,m = 14 or 15 and p,q = 16 or 18)

Molecule	Obsd (cm^{-1})	Calcd (cm^{-1})	Mode	Molecule	Obsd (cm^{-1})	Calcd (cm^{-1})	Mode
$^{16}O_2Pt(^{14}N_2)_2$	897	898.5	ν_{O-O}	$^{16}O_2Pt(^{14}N_2)(^{15}N_2)$	—	898.5	ν_{O-O}
	—	331.1	ν_{M-O} sym		(2261)	2262.9	$\nu_{^{14}N-^{14}N}$
	2267	2266.3	ν_{N-N} sym		(2180)	2185.9	$\nu_{^{15}N-^{15}N}$
	2260	2259.3	ν_{N-N} asym		—	383.2	$\nu_{M-^{14}N}$
	—	387.3	ν_{M-N} sym		—	354.8	$\nu_{M-^{15}N}$
$^{16}O_2Pt(^{15}N_2)_2$	897	898.5	ν_{O-O}	$^{16}O_2Pt(^{14}N^{15}N)_2$	(2231)	2229.0	ν_{N-N} sym
	—	329.2	ν_{M-O} sym		(2225)	2221.8	ν_{N-N} asym
	2188	2189.5	ν_{N-N} sym	$^{16}O_2Pt(^{15}N^{14}N)_2$	(2225)	2227.5	ν_{N-N} sym
	2181	2182.7	ν_{N-N} asym		(2219)	2221.0	ν_{N-N} asym
	—	377.4	ν_{M-N} sym	$^{16}O_2Pt(^{14}N_2)(^{14}N^{15}N)$	(2261)	2263.1	$\nu_{^{14}N-^{14}N}$
$^{18}O_2Pt(^{14}N_2)_2$	848	847.5	ν_{O-O}		(2225)	2225.0	$\nu_{^{14}N-^{15}N}$
	—	315.6	ν_{M-O} sym	$^{16}O_2Pt(^{14}N_2)(^{15}N^{14}N)$	(2261)	2263.1	$\nu_{^{14}N-^{14}N}$
	2267	2266.2	ν_{N-N} sym		(2225)	2224.0	$\nu_{^{15}N-^{14}N}$
	2260	2259.3	ν_{N-N} asym	$^{16}O_2Pt(^{14}N^{15}N)(^{15}N^{14}N)$	2231	2228.3	$\nu_{^{14}N-^{15}N}$
	—	386.0	ν_{M-N} sym		2219	2221.3	$\nu_{^{15}N-^{14}N}$
$^{16}O^{18}OPt(^{14}N_2)_2$	872	873.4	ν_{O-O}	$^{16}O_2Pt(^{14}N^{15}N)(^{15}N_2)$	(2225)	2225.7	$\nu_{^{14}N-^{15}N}$
	2267	2266.3	ν_{N-N} sym		(2189)	2185.8	$\nu_{^{15}N-^{15}N}$
	2260	2259.3	ν_{N-N} asym	$^{16}O_2Pt(^{15}N^{14}N)(^{15}N_2)$	(2225)	2224.5	$\nu_{^{15}N-^{14}N}$
					(2189)	2185.8	$\nu_{^{15}N-^{15}N}$

Table VIII. Best Fit MVFF Force Constants[a] for $(O_2)M(N_2)_2$ (where M = Ni, Pd, or Pt)

	$(O_2)Ni(N_2)_2$	$(O_2)Pd(N_2)_2$	$(O_2)Pt(N_2)_2$
k_{NN}	21.20	22.00	21.30
$k_{NN\cdot NN}$	0.17	0.02	0.02
$k_{NN\cdot OO}$	0.30	0.30	0.30
$k_{MN\cdot NN}$	0.33	0.50	0.70
$k_{MN\cdot MN}$	0.20	0.20	0.20
k_{MN}	1.60	1.80	2.00
$k_{MN\cdot MO}$	0.01	0.01	0.01
k_{OO}	3.88	4.22	3.30
$k_{OO\cdot MO}$	0.38	0.38	0.44
k_{MO}	1.40	1.45	1.10
$k_{MO\cdot MO}$	0.40	0.24	0.22
$k_{MN\cdot OO}$	0.01	0.01	0.01
$k_{NN\cdot MO}$	0.01	0.01	0.01

[a] Units in mdyn/Å.

compounds. This trend is reflected in the respective force constants (Table IX). We have suggested earlier[4,6,7,11] for the parent dinitrogen complexes that the difference between the force constants of free and coordinated dinitrogen can be taken as a rough measure for the weakening of the NN bond. If this idea can be extended to the mixed dioxygen dinitrogen complexes, then one can see that the NN bonds in $(O_2)M(N_2)$ and $(O_2)M(N_2)_2$ are stronger than the stoichiometrically highest $M(N_2)_n$ complex. Although one can probably only make meaningful comparisons within a related group of complexes, one might speculate that $(O_2)M(N_2)$ and $(O_2)M(N_2)_2$ are thermodynamically less stable than their parent $M(N_2)_n$ complexes. The extremely high values of the NN bond stretching force constants, particularly in $(O_2)Pd(N_2)$ and $(O_2)Pd(N_2)_2$, indicate a very weak M-N_2 interaction. In actual fact, these NN stretching frequencies are the *highest* values known so far for coordinated dinitrogen.

Continuing along these lines we note that for the mixed dioxygen dinitrogen complexes the deviation of the NN stretching force constants from the value of free N_2 follows the order Ni > Pt > Pd, which parallels the order previously observed for the parent dinitrogen complexes, $M(N_2)_n$.[4,7]

Table IX. Relevant Frequencies[a] and Bond Stretching Force Constants[b] of Binary and Mixed Binary Dioxygen Dinitrogen Complexes of Nickel, Palladium, and Platinum

		MO_2	MN_2	$M(N_2)_2$	$(O_2)M(N_2)$	$(O_2)M(N_2)_2$
Nickel	ν_{O-O}	966	—		977	972
	ν_{Ni-O}	507	—		478	
	ν_{N-N}	—	—	2187	2243	2283
	ν_{N-N}	—	2089	2106		2260
	ν_{Ni-N}	—	446	406	368	345
	k_{OO}	3.57			3.79	3.88
	k_{NiO}	1.92			1.57	1.40
	k_{NN}		17.62	18.85	20.90	21.2
	$k_{NN\cdot NN}$			0.67		0.16
	k_{NiN}		2.50	1.60	1.78	1.60
	$k_{NN\cdot NiN}$		0.25	0.25	0.59	0.33
Palladium	ν_{O-O}	1024	—	—	1014	998
	ν_{Pd-O}	427	—	—	418	
	ν_{N-N}	—	—	2267		2310
	ν_{N-N}	—	2213	2234	2288	2304
	ν_{Pd-N}	—	378	339	366	
	k_{OO}	4.37			4.29	4.22
	k_{PdO}	1.53			1.48	1.45
	k_{NN}		20.46	21.26	21.91	22.00
	$k_{NN\cdot NN}$			0.27		0.02
	k_{PdN}		1.88	1.38	1.84	1.80
	$k_{NN\cdot PdN}$		0.72	0.72	0.77	0.50
Platinum	ν_{O-O}	925			909	897
	ν_{Pt-O}					
	ν_{N-N}				2229	2267
	ν_{N-N}		2172/2168	2197		2260
	ν_{Pt-N}		394	360	392	
	k_{OO}	3.53			3.37	3.30
	k_{PtO}	1.20			1.20	1.10
	k_{NN}		19.00	20.03	20.91	21.30
	$k_{NN\cdot NN}$			0.43		0.02
	k_{PtN}		2.26	1.87	2.26	2.0
	$k_{NN\cdot PtN}$		0.12	0.12	0.95	0.7

[a] Units in cm^{-1}. [b] Units in mdyn/Å.

We have previously defined a bond energy function ΔH_c by $\Delta H_c = n\Delta F_{NN}$ where $\Delta F_{NN} = k_{NN} - k'_{NN}$, and k_{NN} and k'_{NN} are the free and complexed ligand bond stretching force constants, respectively, and n is the coordination number with respect to the dinitrogen ligand. It was previously speculated that ΔH_c gives a measure of the enthalpy of decomposition of the appropriate compound for which it was measured. The computed values of ΔH_c for the parent $M(N_2)_n$ complexes of Ni, Pd, and Pt as a function of n, as well as the values of ΔH_c for $(O_2)M(N_2)$ and $(O_2)M(N_2)_2$ are shown in Figure 11. The results for all complexes are seen to parallel their warm-up behavior and suggest that the most stable dioxygen dinitrogen complexes are those with the highest N_2 stoichiometry. It is also interesting to note that the order of relative thermodynamic stabilities for $(O_2)M(N_2)$ and $(O_2)M(N_2)_2$ (for M = Ni, Pd, and Pt) is Ni $\simeq$ Pt > Pd which roughly parallels the order of stability of the parent $M(N_2)_n$ complexes, that is, Ni > Pt > Pd.

The bonding properties of the mixed dinitrogen dioxygen complexes are probably best described in terms of dinitrogen coordination toward a binary dioxygen complex, the latter closely approximating an ionic formulation, $M^{\delta+}(O_2^{\delta-})$, where the oxygen is somewhere between peroxide and superoxide in character. In this respect, the $(O_2)M(N_2)$ and $(O_2)M(N_2)_2$ complexes closely resemble DeKock's[12] $(N_2)MF_2$ and $(CO)MF_2$ complexes formed by cocondensing gaseous MF_2 monomers (where M = Cr, Mn, Fe, Co, Ni, and Zn) with the appropriate ligand under conditions of matrix isolation. In particular, DeKock's carbonyl complexes yielded convincing evidence of a bonding situation in which CO acts essentially as a σ-donor to an ionically bound MF_2 moiety. The CO absorptions, without exception, appeared above 2138 cm^{-1}, the frequency of uncoordinated CO. In an ionic stiuation of the type $(CO)M^{2+}(2F^-)$,

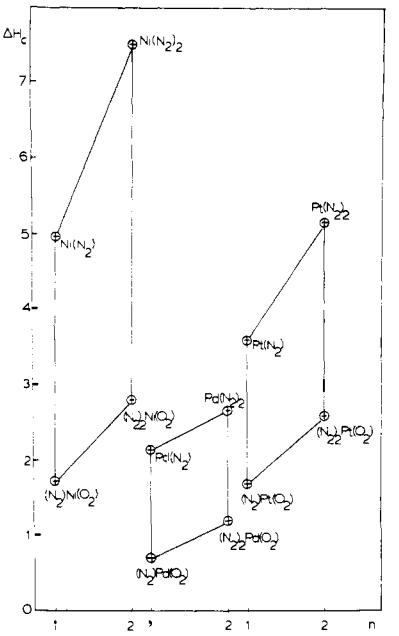

Figure 11. The computed values of ΔH_c as a function of n for $M(N_2)_n$ and $(O_2)M(N_2)_n$ (where M = Ni, Pd, or Pt).

the π-donation of charge from a cationic metal center to the 2π orbitals of CO is greatly diminished compared to a formally uncharged metal center. On the other hand, the σ-donor properties of the CO are considerably enhanced, the outcome being a strengthening of the CO bond (remembering the 5σ donor orbital of CO is slightly antibonding) relative to uncoordinated CO. In fact, recent molecular or-

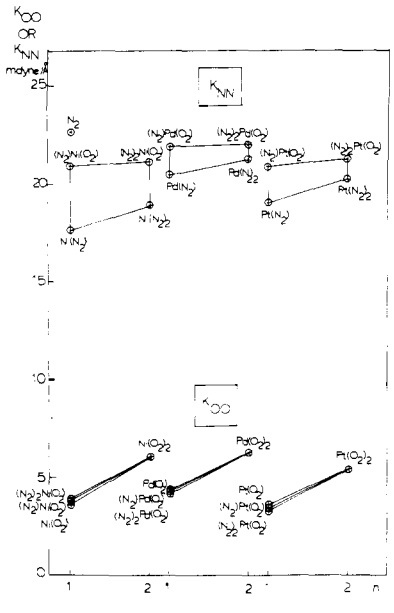

Figure 12. Graphical representation of the k_{NN} and k_{OO} bond stretching force constants for $M(N_2)_n$, $(O_2)M(N_2)_n$, and $M(O_2)_n$ as a function of n (where $n = 1$ or 2).

bital calculations[13] on $Ni^0(CO)$, $Ni^I(CO)$, $Ni^{II}(CO)$, and $Ni^{III}(CO)$ lend strong support to the contention of increasing σ-donor and decreasing π-acceptor participation of the CO ligand to the metal, with increasing oxidation state of the metal.

Assuming that we can carry over these ideas to N_2, it is not surprising on examining the best fit MVFF force constants for $M(N_2)$, $M(N_2)_2$, $M(O_2)$, $(O_2)M(N_2)$, and $(O_2)M(N_2)_2$ (Table IX and Figure 12) that a *large* increase in the k_{NN} force constant is observed on coordinating a single O_2 ligand to MN_2 to form $(O_2)M(N_2)$. In essence, the change reflects a transition from MN_2 in which N_2 bonds in the commonly encountered σ-π synergic manner, to $(N_2)M^{\delta+}(O_2^{\delta-})$ in which the N_2 can be considered to be weakly coordinating in a predominantly σ-type fashion to $M^{\delta+}$ (where $2 \geq \delta^+ \geq 1$), consistent with k_{NN} force constants very close to that of uncoordinated N_2.

The coordination of a second N_2 ligand to yield $(N_2)_2M^{\delta+}(O_2^{\delta-})$ has very little effect other than causing a slight reduction in N_2 σ-bonding with a concomitant marginal increase in k_{NN} compared to that of $(N_2)M^{\delta+}(O_2^{\delta-})$ (Table IX and Figure 12).

Consistent with the proposal of an ionic moiety $M^{\delta+}(O_2^{\delta-})$ to which N_2 weakly coordinates in an approximately σ-bonded fashion are the *marginal* changes observed in the k_{OO} force constants on passing from $M(O_2)$ to $(N_2)M(O_2)$ and $(N_2)_2M(O_2)$ (Table IX and Figure 12). Here, the dioxygen approximately satisfies the charge requirements of the metal and barely senses the presence of weakly interacting N_2 ligands. On the other hand, a *large* increase in k_{OO} is observed when a second dioxygen is coordinated to $M(O_2)$ to yield $M(O_2)_2$ (Figure 12), an effect which probably reflects a transition from $M^{\delta+}(O_2^{\delta-})$, in which δ is closer to peroxide character, to $M^{2\delta+}(O_2^{\delta-})_2$, in which δ is closer to superoxide character.

Summary

Using matrix isolation techniques, it has proven possible to synthesize for the first time binary mixed dioxygen dinitrogen complexes of nickel, palladium, and platinum. Isotopic substitution at the nitrogen and oxygen characterize the complexes to be $(O_2)M(N_2)$ and $(O_2)M(N_2)_2$, the dioxygen bonded in a side-on fashion, the dinitrogen in an end-on fashion.

The vibrational studies and force constant calculations enable one to gain a unique insight into the simultaneous bonding properties of N_2 and O_2 to a common metal atom, where the ligands can be considered to be competing for the same valence electrons. The overall bonding picture that emerges for $(O_2)M(N_2)$ and $(O_2)M(N_2)_2$ is an unusual situation in which N_2 weakly coordinates in a predominantly σ-type fashion to a metal dioxygen moiety probably best formulated as $M^{\delta+}(O_2^{\delta-})$. The O_2 ligand is probably somewhere between peroxide and superoxide in character.

Hopefully, the discovery that mixed dioxygen dinitrogen complexes of the nickel group are capable of an independent existence will stimulate synthetic chemists to search for more stable dioxygen dinitrogen complexes and investigate their relationship, if any, to those biological systems that are able to fix dinitrogen in an aerobic environment. It is not inconceivable that dinitrogen dioxygen complexes are involved in these reactions, especially those complexes that are deactivated by the presence of dioxygen.

Acknowledgments. We wish to thank the National Research Council of Canada and the Research Corporation for financial assistance. W. K. gratefully acknowledges a scholarship from the Deutscher Akademischer Austauschdienst.

References and Notes

(1) W. Klotzbücher and G. A. Ozin, *J. Am. Chem. Soc.*, **95**, 3790 (1973).
(2) E. P. Kündig, M. Moskovits, and G. A. Ozin, *J. Mol. Struct.*, **14**, 137 (1972).
(3) (a) M. Moskovits and G. A. Ozin, *J. Appl. Spectrosc.*, **26**, 481, 1972; (b) G. Schachtschneider, "Vibrational Analysis of Polyatomic Molecules", Shell Development Co., Emeryville, Calif., 1964.
(4) E. P. Kündig, H. Huber, M. Moskovits, and G. A. Ozin, *J. Am. Chem. Soc.*, **95**, 332 (1973).
(5) H. Huber, W. Klotzbücher, G. A. Ozin, and A. Vander Voet, *Can. J. Chem.*, **51**, 2722 (1973).
(6) E. P. Kündig, M. Moskovits, and G. A. Ozin, *Can. J. Chem.*, **51**, 2710 (1973); D. W. Green, J. Thomas, and D. M. Gruen, *J. Chem. Phys.*, **58**, 5453 (1973).
(7) W. Klotzbücher and G. A. Ozin, *J. Am. Chem. Soc.*, in press.
(8) G. A. Ozin and A. Vander Voet, *Acc. Chem. Res.*, **6**, 313 (1973).
(9) M. Moskovits and G. A. Ozin, *J. Chem. Phys.*, **58**, 1251 (1973).
(10) F. A. Cotton and C. S. Kralhanzel, *J. Am. Chem. Soc.*, **84**, 4432 (1962).
(11) E. P. Kündig, D. McIntosh, M. Moskovits, and G. A. Ozin, *J. Am. Chem. Soc.*, **95**, 7234 (1973).
(12) C. W. Dekock and D. A. Van Liersburg, *J. Am. Chem. Soc.*, **94**, 3235 (1972); *J. Phys. Chem.* **78**, 134 (1974).
(13) P. Politzer and S. D. Kasten, *Surf. Sci.*, **36**, 186 (1973).